Reactions of pyridyl donors with halogens and interhalogens: an X-ray diffraction and FT-Raman investigation

M. Carla Aragoni [a], Massimiliano Arca [a,*], Francesco A. Devillanova [a], Michael B. Hursthouse [b], Susanne L. Huth [b], Francesco Isaia [a], Vito Lippolis [a], Annalisa Mancini [a], Helen R. Ogilvie [b], Gaetano Verani [a]

[a] *Dipartimento di Chimica Inorganica ed Analitica, Università degli Studi di Cagliari, S.S. 554 bivio per Sestu, 09042 Monserrato – Cagliari, Italy*
[b] *School of Chemistry, University of Southampton, Highfield, Southampton SO17 1BJ, UK*

Abstract

Three different N-donors **L**, namely *N*-ethyl-*N'*-3-pyridyl-imidazolidine-4,5-dione-2-thione (**1**), *N,N'*-bis(3-pyridylmethyl)-imidazolidine-4,5-dione-2-thione (**2**), and tetra-2-pyridyl-pyrazine (**3**), bearing one, two and four pyridyl substituents, respectively, have been reacted with halogens X_2 (X = Br, I) or interhalogens XY (X = I; Y = Cl, Br). CT σ–adducts **L** · nXY, bearing linear N···XY moieties (**L** = **3**; X = I; Y = Br, I; $n = 2$), and salts containing the protonated cationic donors H_nL^{n+} (**L** = **1** − **3**; $n = 1, 2, 4$), counterbalanced by Cl^-, Br^-, I_3^-, Br_3^-, I_5^-, Br_5^-, I_2Br^-, $I_3Br_4^-$, or ICl_2^- anions, have been isolated. Among the reactions products, $(H\mathbf{1}^+)Cl^-$, $(H\mathbf{1}^+)Br^-$, $(H\mathbf{2}^+)I_3^-$, $(H_2\mathbf{3}^{2+})(ICl_2^-)_2$, and **3** · 2IBr have been characterised by single-crystal X-ray diffraction. The nature of the products has been elucidated based on elemental analysis and FT-Raman spectroscopy supported by MP2 and DFT calculations.
© 2004 Elsevier B.V. All rights reserved.

Keywords: Pyridyl donors; Halides; CT-adducts; FT-Raman; X-ray crystal structures

1. Introduction

All discrete and extended polyhalides can be considered as originated by the interaction of X^-, X_2, and X_3^- building blocks (X = Cl, Br, I) [1]. The tendency of halogens to catenate and form extended polyanions with general formula X_{2m+n}^{n-} $(n, m > 0)$ increases on passing from chlorine to iodine [2]. Thus, while a large number of discrete polyiodides [2,3], up to I_{29}^{3-} [4], and some examples of infinite networks [5,6] are known, only few extended polybromides, such as Br_4^{2-} [7,8] and Br_8^{2-} [9], and only one case of infinite polybromide network

[10] have been characterised in the solid state. The nature of the component building blocks is reflected in the Raman response of the assembled frameworks, since all polyhalide and polyhalogen networks show Raman peaks related to the vibrational modes of X_2 and X_3^- building blocks perturbed by X···X and/or X···donor interactions [5,11,12].

In all cases, the nature (size, shape and charge) of the templating cation has been recognised to be crucial in determining the extension as well as the structural and geometrical features of polyhalide species [5,6]. In this context, the reactivity of heterocyclic N-bases **L**, such as pyridine (Py) and 1,4-diazine derivatives, with halogen and interhalogens has attracted an increasing interest during the last decades, in virtue of the ability of these substrates both to behave as σ-donors to give

---

neutral charge-transfer (CT) adducts and to undergo N-protonation, the resulting cations being counterbalanced by discrete or extended polyhalides frameworks. The vast majority of the products characterised in the literature refers to the reactions of donors of type **L** with I_2 [13]. In particular, not only a large number of neutral charge-transfer adducts **L·I_2** featuring N–I–I linear groups (**L** = variously substituted pyridine and derivatives [14], such as 2,2′- and 4,4′-bipyridine (bipy), pyrazine and derivatives [15–17], and acridine [18]) and cationic N-protonated products HL$^+$ counterbalanced by iodide anions or polyiodide networks [6] has been reported, but also N-iodopyridinium ions LI$^+$ [19], two nitrogen donors coordinated to iodine(I) complexes (**L–I–L**)$^+$ [20], and diiodine molecules bridging two donor units **L–I–I–L** have been described. Protonated cations were found also under anhydrous conditions, but the protonation mechanism was not much investigated [13]. In the case of pyridine, it has been hypothesised that the first reaction product would be a CT adduct **L·I_2**. This would be in equilibrium with the ion pair LI$^+$I$^-$ [13,21], thus accounting for the isolation of reaction products containing N-iodopyridinium ions. On the other side, the oxidation of the aromatic heterocycle to give cationic radical species (**L·**)$^+$ has been proposed to be responsible for the formation of stable cationic protonated species by solvolysis or reaction with incipient moisture [13]. Though less investigated, the reactions of donors **L** with Br_2, IBr and ICl also yield both CT-adducts and protonated HL$^+$ species, balanced by different types of polyhalides. As an example, from the reaction of 2,2′-bipy with IBr both the neutral CT adduct 2,2′-bipy·2IBr [22], and the salts [H(2,2′-bipy)$^+$](H$_3$O$^+$)(IBr$_2^-$)$_2$, or [H(2,2′-bipy)$^+$](I$_2$Br$_3^-$) [23] were obtained, depending on the reaction conditions.

Following our previous investigations on chalcogen donors towards halogens [1,24,25], interhalogens [26], and the *pseudo*-halogen ICN [27], and encouraged by the recent results obtained with di-[2]-pyridyl-disulfide, which was able to template an infinite polyiodide 3D-network [6], we are systematically testing the reactivity towards halogens and interhalogens of polypyridyl donors, differing in their dimensions, conformations, and directionality of N-donor sites.

In this paper we report the synthesis and the solid-state FT-Raman characterisation of the products obtained by reacting N-ethyl-N′-3-pyridyl-imidazolidine-4,5-dione-2-thione (**1**) [28], N,N′-bis(3-pyridyl-methyl)-imidazolidine-4,5-dione-2-thione (**2**) [28], and tetra-2-pyridyl-pyrazine (**3**), containing one, two, and four pyridyl donors, respectively (Chart 1), with I_2, Br_2, IBr and ICl. Some of these reaction products have been also characterised by single crystal X-ray diffraction.

2. Result and discussion

2.1. Synthesis of 1–3 and reactivity towards halogens and interhalogens

N-Ethyl-N′-3-pyridyl-imidazolidine-4,5-dione-2-thione (**1**) and N,N′-bis(3-pyridylmethyl)-imidazolidine-4,5-dione-2-thione (**2**) were synthesised by reacting N-ethyl-N′-3-pyridyl-thiourea and N,N′-bis(3-pyridylmethyl)thiourea, respectively, with oxalyl chloride, according to the procedure previously outlined for different thioparabanic acid derivatives [29]. Tetra-2-pyridyl-pyrazine (**3**) was obtained according to literature methods [30]. **1**–**3** have been reacted in methylene chloride with I_2, Br_2, IBr, and ICl in donor:acceptor molar ratios ranging between 1:0.5 and 1:5, obtaining the solid-state products summarised in Table 1. The products have been characterised by means of elemental analyses, FT-IR and FT-Raman spectroscopy, and X-ray diffraction when suitable crystals were available [31].

An examination of the stoichiometries of the reaction products listed in Table 1 shows that in several cases a unique product was obtained for all molar ratios, and that products rich in halogen were isolated even when **1**–**3** were reacted with stoichiometrically defective amounts of halogens. This indicates the particular stability of the products isolated in the solid state, attributable to the formation of ionic species further stabilised in networks build up through hydrogen or halogen bridging.

2.2. Crystal structure determinations

Among the fifteen different reaction products summarised in Table 1, six have been characterised by single crystal X-ray diffraction. In addition, the crystal structure of **1** has been obtained. The crystal data for **1**,
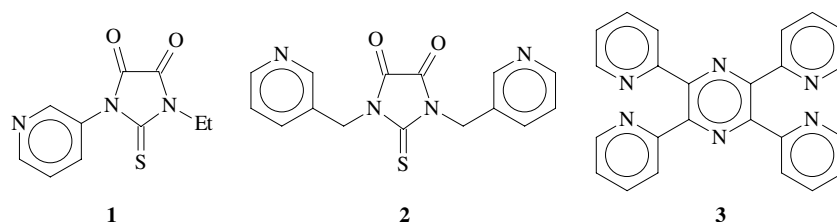

Chart 1.

Table 1
Stoichiometry and main FT-Raman peaks (50–500 cm^{-1})[a] of the products obtained by reacting pyridyl donors **L** (1–3) with halogens and interhalogens XY (XY = I$_2$, Br$_2$, IBr and ICl) in molar ratios L:XY ranging between 1:0.5 and 1:5

L	L:XY ratio	XY							
		I$_2$		Br$_2$		IBr		ICl	
		Product	FT-Raman	Product	FT-Raman	Product	FT-Raman	Product	FT-Raman
1	1:0.5	(H**1**$^+$)I$_5^-$	160 (10.0)	(H**1**$^+$)Br^{-c}	–	(H**1**$^+$)I$_2$Br$^-$	139 (5.7)	(H**1**$^+$)Cl^{-c}	–
	1:1		111 (4.8)	(H**1**$^+$)Br$_5^-$	176 (9.9)		120 (10.0)	(H**1**$^+$)ICl$_2^-$	271 (10.0)
	1:2				160 (10.0)		82.0 (1.8)		85 (5.7)
	1:5				78 (2.7)				
2	1:0.5	(H**2**$^+$)I$_3^{-c}$	115 (10.0)	(H**2**$^+$)Br$_5^-$	191 (10.0)	(H**2**$^+$)I$_3$Br$_4^-$	223 (6.6)	(H$_2$**2**$^{2+}$)(ICl$_2^-$)$_2$	268 (10.0)
	1:1				157 (8.3)		213 (6.6)		84 (8.0)
	1:2				81 (6.5)		186 (10.0)		
	1:5								
3	1:0.5	(**3**·2I$_2$) : [(H**3**$^+$)I$_3^-$]	170 (10.0)	(H**3**$^+$)Br$_3^-$	160 (10.0)	**3**·2IBr^c	204 (10.0)	(H$_2$**3**$^{2+}$)(ICl$_2^-$)$_2^{c}$	267 (10.0)
	1:1	1:1 mixture[b]	147 (5.7)		167 (10.0)[d]				86 (6.6)
	1:2		110 (4.1)	(H$_4$**3**$^{4+}$)(Br$_4^{2-}$)					
	1:5			(Br$^-$)$_2$[d]					

[a] Only main peaks are reported.
[b] The adduct **3**·2I$_2$ was reported in [17].
[c] Crystal structure reported in this paper.
[d] See [8].

(H**1**$^+$)Br$^-$, (H**1**$^+$)Cl$^-$, (H**2**$^+$)I$_3^-$, **3**·2IBr, and (H$_2$**3**$^{2+}$)(ICl$_2^-$)$_2$ are summarised in Table 2, while the structure of (H$_4$**3**$^{4+}$)(Br$_4^{2-}$)(Br$^-$)$_2$ has been recently reported elsewhere [8]. The crystal structure of **1** does not present any new points of interest compared to those of the other thioparabanic acid derivatives reported previously [32,33]. The structures of (H**1**$^+$)Br$^-$ and (H**1**$^+$)Cl$^-$ also do not require further comments, except for the fact that in both salts the pyridine unit, twisted by 73.21° and 78.38°, respectively, with respect to the planar imidazolidine ring, is protonated at the nitrogen atom and the charge of the resulting cation H**1**$^+$ is balanced by a bromide and a chloride anion, respectively.

The crystal structure of (H**2**$^+$)I$_3^-$ is shown in Fig. 1. In this compound, **2** is protonated at the N(3) atom of a 3-pyridylmethyl substituent, with the two substituents at the imidazolidine ring folded to embrace the almost symmetric linear I$_3^-$ anion [I(1)–I(2), 2.9037(7); I(1)–I(3), 2.9150(7) Å; I(2)–I(1)–I(3), 176.97(2)°], while C–H···O [C(4)–H(4A)···O(1), 2.469 and C(8)–H(8)···O(2), 2.628 Å, respectively] and C–H···S contacts [C(15)–H(15)···S(1), 2.807 Å] are responsible for the crystal packing.

The CT-adduct **3**·2IBr, isolated from the reactions of **3** and IBr in all molar ratios (Fig. 2), presents a structure comparable to that of **3**·2I$_2$, though, due to the

Table 2
Crystal data for **1**, (H**1**$^+$)Br$^-$, (H**1**$^+$)Cl$^-$, (H**2**$^+$)I$_3^-$, **3**·2IBr and (H$_2$**3**$^{2+}$)(ICl$_2^-$)$_2$[a]

	1	(H**1**$^+$)Br$^-$	(H**1**$^+$)Cl$^-$	(H**2**$^+$)I$_3^-$	**3**·2IBr	(H$_2$**3**$^{2+}$)(ICl$_2^-$)$_2$
Empirical formula	C$_{10}$H$_9$N$_3$O$_2$S	C$_{10}$H$_{10}$N$_3$O$_2$SBr	C$_{10}$H$_{10}$N$_3$O$_2$SCl	C$_{15}$H$_{13}$N$_4$O$_2$SI$_3$	C$_{24}$H$_{16}$N$_6$Br$_2$I$_2$	C$_{24}$H$_{18}$N$_6$Cl$_4$I$_2$
Crystal size (mm)	0.12 × 0.16 × 0.16	0.14 × 0.22 × 0.24	0.15 × 0.15 × 0.24	0.42 × 0.38 × 0.18	0.20 × 0.40 × 0.65	0.02 × 0.08 × 0.15
Crystal system	Monoclinic	Monoclinic	Monoclinic	Orthorhombic	Orthorhombic	Orthorhombic
Space group	P_1/n	P_1/c	P_1/c	Pbca	Pna2$_1$	Pbca
a (Å)	9.6772(10)	7.9845(9)	7.9042(9)	12.5430(3)	14.8732(11)	7.1213(3)
b (Å)	5.5348(8)	14.5464(16)	14.7357(6)	13.7339(4)	7.4817(4)	15.4460(6)
c (Å)	19.080(4)	10.8260(9)	10.4051(15)	24.3159(7)	23.3222(13)	24.2383(7)
α (°)	90	90	90	90	90	90
β (°)	97.024(9)	99.620(9)	99.031(10)	90	90	90
γ (°)	90	90	90	90	90	90
V (Å^3)	1014.3(3)	1239.7(2)	1196.9(2)	4188.8(2)	2595.2(3)	2666.11(17)
Z	4	4	4	8	4	4
D_{calc} (Mg m^{-3})	1.541	1.694	1.508	2.201	2.053	1.958
Independent reflections	2312	2813	2736	4674	5758	3028
Number of parameters	182	195	195	267	329	195
Final R indices[b]	0.0341	0.0259	0.0410	0.0423	0.0207	0.0449
wR$_2$ (all data)	0.0814	0.0679	0.1078	0.0972	0.0469	0.0871

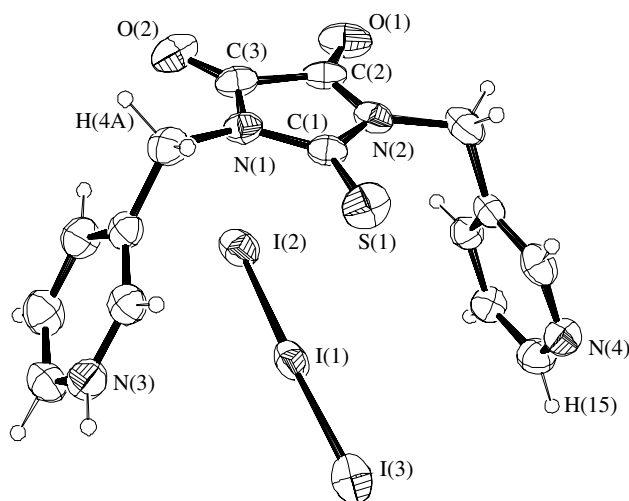[a] T = 120(2) K. Wavelength Mo Kα (0.71073 Å).
[b] [$F^2 > 2\sigma(F^2)$].

Fig. 1. ORTEP drawing and atom-labelling scheme for $(H2^+)(I_3^-)$. Hydrogen atoms involved in hydrogen bridging have been labelled. Selected bond lengths (Å) and angles (°): I(1)–I(2) 2.9037(7), I(1)–I(3) 2.9150(7), C(1)–N(1) 1.368(7), C(1)–N(2) 1.398(7), C(1)–S(1) 1.593(5), C(3)–N(1) 1.372(8), C(2)–N(2) 1.364(9), C(2)–O(1) 1.196(8), C(2)–C(3) 1.526(9), C(3)–O(2) 1.211(8) Å; I(2)–I(1)–I(3) 176.98(2)°.

higher acidity of IBr with respect to I_2, the two IBr molecules are more strongly bonded to two pyridyl units in **3 · 2IBr** than the two I_2 in **3 · 2I$_2$** [N(3)···I(1), 2.405(3); N(5)···I(2), 2.410(3) Å for the former adduct, as compared to 2.562(8) Å found for both N···I distances for the latter] [17]. The I–Br distances [I(1)–Br(1), 2.5952(4); I(2)–Br(2), 2.5878(5) Å], elongated compared to those found in solid IBr [2.521(4) Å] [34], are similar to those found in 2,2′-bipy · 2IBr [d(I–Br), 2.58 Å] [22]. It is worthy of note that the elongation in the I–Br bond distances (0.074 and 0.067 Å for the two IBr units) is considerably smaller than that found in the CT-adducts
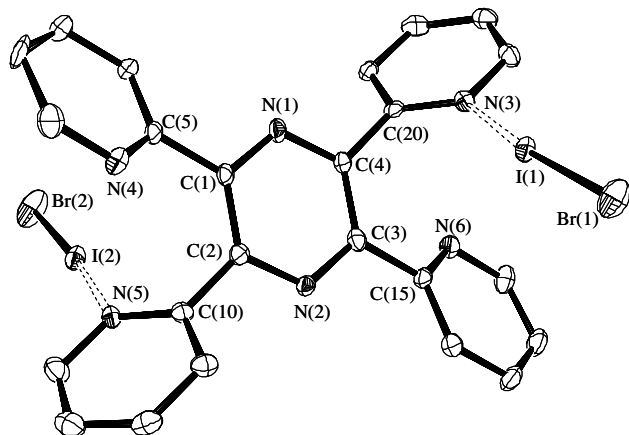
between IBr and chalcogen donors (average elongation values in the IBr distances based on an examination of the CCDC database: thioethers, 0.154; thiocarbonyl donors, 0.192; selenoethers, 0.198; selenocarbonyl donors, 0.340 Å), and classifies **3 · 2IBr** as a weak adduct [35]. The N···I–Br bond angles are slightly bent [N(3)–I(1)–Br(1), 173.99(6); N(5)–I(2)–Br(2), 175.14(6)°], as is typical of this family of compounds [17]. The bond lengths and angles within the donor moiety are rather unperturbed upon complexation, the values being very close to those found in the crystal structure of **3 · 2I$_2$** and of the monoclinic polymorph of **3** [17,36], with the pyridyl substituents assuming an *endo, endo* conformation, with nitrogen atoms of adjacent pyridine rings laying on opposite sides with respect to the pyrazine ring plane. As in the case of **3 · 2I$_2$**, the pyridine rings bound to the halogen are more rotated [C(3)–C(4)–C(20)–N(3), 57.0(4); C(1)–C(2)–C(10)–N(5), 56.5(4); for **3 · I$_2$**, 56.1°] than the free ones [C(2)–C(1)–C(5)–N(4), 30.6(4); C(4)–C(3)–C(15)–N(6), 27.9(4); for **3 · I$_2$**, 28.5°] with respect to the pyrazine core.

The reaction of **3** with ICl in all the explored molar ratios gave the salt $(H_2 3^{2+})(ICl_2^-)_2$, whose crystal structure (Fig. 3) shows the diprotonated dication $H_2 3^{2+}$ counterbalanced by two symmetry-related ICl_2^- anions [I(1)–Cl(1), 2.5555(15); I(1)–Cl(2), 2.5360(60) Å]. The dication assumes the conformation found in $(H_2 3^{2+})[B(C_6H_5)_4^-]_2$ [37]. The formation of *intra* molecular N(1)–H(1N)···N(2) hydrogen bonds forces the organic donor into a flattened structure [N(1)–C(5)–C(6)–C(7), 23.9(9); N(2)–C(8)–C(7)–C(6), 23.9(9)°] with the nitrogen atoms of vicinal pyridine rings oriented two

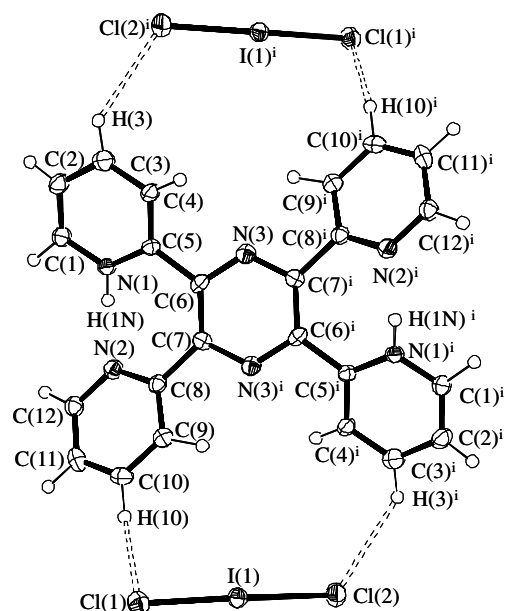Fig. 2. ORTEP drawing and atom labelling scheme for the compound **3 · 2IBr**. Hydrogen atoms have been omitted for clarity. Selected bond lengths and angles: I(1)–Br(1) 2.5952(4), I(2)–Br(2) 2.5878(5), N(3)–I(1) 2.405(3), N(5)–I(2) 2.409(3) Å; N(3)–I(1)–Br(1) 173.99(6), N(5)–I(2)–Br(2) 175.14(6), C(1)–C(2)–C(10)–N(5) 56.51, C(3)–C(4)–C(20)–N(3) −57.02°.

Fig. 3. ORTEP drawing and atom labelling scheme for $(H_2 3^{2+})(ICl_2^-)_2$. Bond lengths and angles for the ICl_2^- anion: I(1)–Cl(1) 2.5555(15), I(1)–Cl(2) 2.5360(15) Å; Cl(1)–I(1)–Cl(2) 174.87(5)°. ^{i} = 1 − x, 1 − y, 1 − z.

above and two below the pirazine plane, and N$\cdots$N distances just 2.528 Å apart (N–H$\cdots$N angle 149.1°). As observed for $(H_2\mathbf{3}^{2+})[B(C_6H_5)_4^-]_2$, these N–H$\cdots$N bridges are rather short even for proton sponges [8,37], and result in a deformation of the C(5)–C(6)–C(7) and C(6)–C(7)–C(8) angles, which are expanded to the very unusual values of 129.7(5) and 130.4(5)°. The $H_2\mathbf{3}^{2+}$ dication interacts with the ICl_2^- anions through an extended network of hydrogen bonds [C(10)–H(10)$\cdots$Cl(1), C(3)^i–H(3)$^i\cdots$Cl(2), C(3)^{ii}–H(3)$^{ii}\cdots$Cl(2), C(1)^{iii}–H(1)$^{iii}\cdots$Cl(1), C(12)^{iii}–H(12)$^{iii}\cdots$Cl(1), C(3)^i–H(3)$^i\cdots$Cl(2)^{iv}; $^i = 1 - x, 1 - y, 1 - z$; $^{ii} = x, -1 + y, z$; $^{iii} = 1 - x, -1/2 + y, 3/2 - z$; $^{iv} = 1-x, -y, 1 - z$], thus defining a waved 2D-framework along the *bc* plane (Fig. 4).

2.3. FT-Raman spectroscopy

It is well known that the formation of CT-adducts between Lewis bases and dihalogens or interhalogens X–Y results in the weakening of the X–Y bond. In the case of weak or medium-weak adducts, this is reflected in the lowering of the frequency of the Raman-active X–Y stretching vibration, thus making this spectroscopy irreplaceable for the characterisation of this type of products. Also in the case of polyiodides, the FT-Raman spectroscopy has been extensively used as a tool able to give useful hints on their structure, since it provides structural information on their X_2 and X_3^- building blocks [3,5,11]. Therefore, solid-state FT-Raman spectra have been recorded for all the products isolated from the

reactions between **1–3** and I_2, Br_2, IBr and ICl (Table 1). In addition, the experimental positions of the FT-Raman peaks have been compared to those calculated at MP2 and DFT/mPW1PW level (Table 3) on all the species suggested by the elemental analyses of the isolated reaction products.

Symmetric linear triiodides (point group $D_{\infty h}$) feature a single Raman-active mode due to the σ_g centrosymmetric stretching vibration close to 110 cm^{-1} (calculated at 109 and 108 cm^{-1} at MP2 and DFT/mPW1PW level, respectively), and two IR-active modes at about 140 and 75 cm^{-1} (calculated at about 135 and 60 cm^{-1}, respectively), due to the σ_u antisymmetric stretching and π_u bending modes, respectively [38]. As I_3^- becomes asymmetric, all the three modes become Raman-active, the intensities of the σ_u and π_u modes increasing with the asymmetry of I_3^- [38]. Highly asymmetric I_3^- ions can be regarded as CT adducts between I^- and I_2 systems, and consequently their FT-Raman spectra show only one strong band in the range 150–180 cm^{-1}, whose position depends on the extent of the perturbation of the I_2 molecule [12].

In the case of higher polyiodides, FT-Raman cannot provide detailed structural information on the topology of the anions, since the technique is capable of detecting only the presence of I_3^- anions and perturbed I_2 molecules, along with some information on the extent of distortion and deformation of these two units, respectively [3,5]. Nonetheless, the use of FT-Raman spectroscopy combined to elemental analysis can be of great help in hypothesising the nature of the reaction products
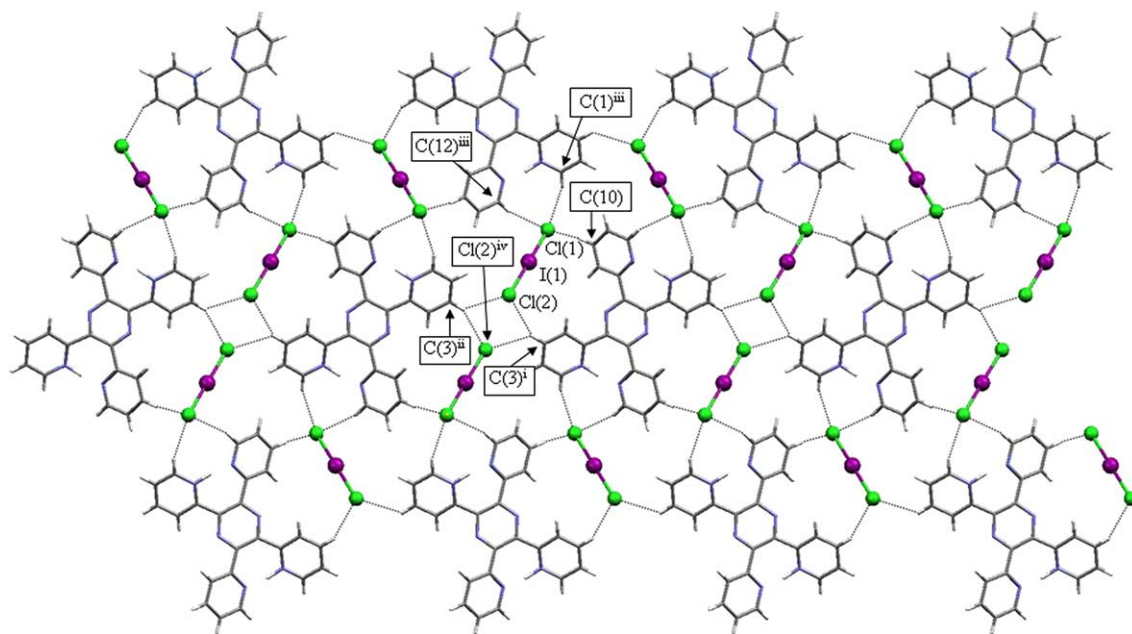

Fig. 4. Self-assembled 2D-framework in $(H_2\mathbf{3}^{2+})(ICl_2^-)_2$. Atoms involved in the hydrogen bridging responsible for the network formation have been labelled. Selected contact distances: H(10)$\cdots$Cl(1) 2.59(5), H(1)$^{iii}\cdots$Cl(1) 2.78(5), H(12)$^{iii}\cdots$Cl(1) 2.70(6), H(3)$^{ii}\cdots$Cl(2) 2.81(8), H(3)$^i\cdots$Cl(2) 2.78(7) Å. $^{ii} = x, -1 + y, z$; $^{iii} = 1 - x, -1/2 + y, 3/2 - z$; $^{iv} = 1 - x, -y, 1 - z$.

Table 3
Optimised distances[a] and normal mode frequencies v(cm^{-1}) calculated at MP2[b] and DFT/mPW1PW[c] levels for halogens (I_2, Br_2) and interhalogens (IBr, ICl) reacted with N-donors **1–3**, and for the polyhalide anions (point group in parentheses) identified in the reaction products summarised in Table 2

			$r_1{}^a$	$r_2{}^a$	v (cm^{-1})
Br_2	$(D_{\infty h})$	b	2.320		326[d]
		c	2.320		323[d]
I_2	$(D_{\infty h})$	b	2.693		220[d]
		c	2.683		221[d]
IBr	$(C_{\infty v})$	b	2.505		271[d]
		c	2.502		270[d]
ICl	$(C_{\infty v})$	b	2.350		381[d]
		c	2.350		380[d]
I_3^-	$(D_{\infty h})$	b	2.988		58 π_u, 109 $\sigma_g{}^d$, 134 σ_u
		c	2.979		57 π_u, 108 $\sigma_g{}^d$, 135 σ_u
Br_3^-	$(D_{\infty h})$	b	2.626		89 π_u, 156 $\sigma_g{}^d$, 181 σ_u
		c	2.628		87 π_u, 154 $\sigma_g{}^d$, 180 σ_u
I_2Br^-	$(D_{\infty h})$	b	2.834		69 π_u, 112 $\sigma_g{}^d$, 162 σ_u
		c	2.826		68 π_u, 112 $\sigma_g{}^d$, 152 σ_u
I_2Br^-	$(C_{\infty v})$	b	2.789	2.969	67 π, 124 σ^d, 155 σ^d
		c	2.793	2.959	65 π, 124 σ^d, 156 σ^d
IBr_2^-	$(D_{\infty h})$	b	2.774		76 π_u, 153 $\sigma_g{}^d$, 163 σ_u
		c	2.776		73 π_u, 150 $\sigma_g{}^d$, 167 σ_u
IBr_2^-	$(C_{\infty v})$	b	2.650	2.810	79 π, 131 σ^d, 174 σ
		c	2.652	2.801	77 π, 130 σ^d, 168 σ
ICl_2^-	$(D_{\infty h})$	b	2.607	2.607	109 π_u, 218 σ_u, 249 $\sigma_g{}^d$
		c	2.608	2.608	110 π_u, 231 σ_u, 247 $\sigma_g{}^d$
Br_5^-	$(D_{\infty h})$	b	2.454	2.818	60 π_u, 71 σ_g, 73 π_g, 98 σ_u, 199 σ_u, 231 $\sigma_g{}^d$
		c	2.465	2.795	42 π_u, 70 π_g, 73 σ_g, 133 σ_u, 201 σ_u, 232 $\sigma_g{}^d$
Br_5^-	(C_{2v})	b	2.478	2.782	10 a_1, 74 b_2, 79 a_2, 82 a_1, 87 b_1, 117 $b_2{}^d$, 126 a_1, 190 $b_2{}^d$, 222 $a_1{}^d$
		c	2.492	2.756	12 a_1, 75 b_2, 78 a_2, 83 a_1, 85 b_1, 129 b_2, 138 a_1, 194 $b_2{}^d$, 221 $a_1{}^d$
I_5^-	$(D_{\infty h})$	b	2.829	3.168	36 π_u, 47 π_g, 51 σ_g, 87 σ_u, 142 σ_u, 163 $\sigma_g{}^d$
		c	2.827	3.137	24 π_u, 45 π_g, 53 σ_g, 101 σ_u, 146 σ_u, 165 $\sigma_g{}^d$
I_5^-	(C_{2v})	b	2.854	3.128	7 a_1, 50 b_2, 52 a_2, 57 a_1, 58 b_1, 91 $a_1{}^d$, 94 b_2, 137 $b_2{}^d$, 158 $a_1{}^d$
		c	2.858	3.137	9 a_1, 50 b_2, 51 a_2, 56 b_1, 58 a_1, 92 $a_1{}^d$, 102 b_2, 141 $b_2{}^d$, 157 $a_1{}^d$

[a] $r_1 \leqslant r_2$.
[b] MP2/LanL2DZdp + ECP.
[c] DFT mPW1PW/LanL2DZdp + ECP.
[d] Intense Raman-active mode (Raman scattering activity > 20 Å^4 amu^{-1}).

obtained from the reactions between halogens and molecular donors.

Among the products obtained by reacting **1–3** with diiodine, $(H2^+)I_3^-$ has been characterised by X-ray diffraction and **3** · $2I_2$ was previously reported [17]. The assignment of the Raman peaks for $(H2^+)I_3^-$ is straightforward: the unique peak at 115 cm^{-1} is indicative of a symmetric triiodide ion, as confirmed by the crystal structure. Slightly more complex is the case of the product obtained by reacting **3** with I_2, whose elemental analysis corresponds to a 1:1 mixture of the CT-adduct **3** · $2I_2$ and of the salt $(H3^+)I_3^-$. Accordingly, the three Raman peaks support the presence of slightly perturbed diiodine (170 cm^{-1}) and asymmetric triiodide (147 and 110 cm^{-1}) [3,38].

The product obtained from **1** and I_2 in all molar ratios presents an elemental analysis compatible with the stoichiometry $(H1^+)I_5^-$, which should contain the cation $H1^+$ protonated at the nitrogen atom of the pyridine ring, as found in the crystal structures of $(H1^+)Br^-$ and $(H1^+)Cl^-$, counterbalanced by a negative charge carried by five iodine atoms. For pentaiodides, both the linear $(D_{\infty h})$ and the bent (C_{2v}) conformations are possible [2], though, according to both MP2 and DFT calculations, the latter is more stable (by about 4.6 kcal/mol at DFT/mPW1PW level), so that authentic examples of the former type, such as in the case of [trimesic acid · H_2O]$_{10}$ $(H^+)(I_5^-)$ [39], are rare. In the case of $(H1^+)I_5^-$, FT-Raman spectroscopy gives a valid help in hypothesising the nature of I_5^-. In fact, the two FT-Raman peaks at 111 and 160 cm^{-1} indicate the presence of both a symmetric I_3^- ion and a perturbed diiodine. However, it is impossible to deduce if these two building blocks are interacting to each other, in which case the resulting pentaiodide should be formulated as I_3^- · I_2.

The reactions of **1–3** with the more oxidising dibromine led in all cases to the protonation of the pyridyl units, the cations being balanced by bromide or polybromide anions. In the case of **3**, two different products were obtained depending on the reaction molar ratio.

By reacting **3** and Br_2 in 1:0.5 or 1:1 molar ratios, a product having stoichiometry $(H3^+)Br_3^-$ was obtained, featuring a single intense FT-Raman peak at 160 cm^{-1}, which can be assigned to the σ_g-stretching mode of a symmetric ($D_{\infty h}$) tribromide, calculated at about 155 cm^{-1} (Table 3). When higher molar ratios were used, $(H_4 3^{4+})(Br_4^{2-})(Br^-)_2$, whose crystal structure has been recently reported [8], was isolated. In this product the FT-Raman peak at 167 cm^{-1} was attributed to the Br–Br stretching of the internal bromine atoms of the Br_4^{2-} anion [8].

Both in the case of **1** and **2**, the monoprotonated cations are balanced by Br_5^- anions featuring three FT-Raman peaks [falling at 176, 160, and 78 cm^{-1} for $(H1^+)Br_5^-$; 191, 157, 81 cm^{-1} for $(H2^+)Br_5^-$]. The frequencies of the three peaks suggest that the anions are bent Br_5^- of the type $Br_3^- \cdot Br_2$.

Among the three products obtained by reacting **1–3** with IBr only **3**·2IBr has been structurally characterised (Fig. 3; see above). Since the two I–Br distances are nearly identical, the FT-Raman peak at 204 cm^{-1} can be assigned to the symmetric combination of the stretching vibrations of the two slightly perturbed IBr molecules. As expected, the value of the vibration frequency reflects the smaller elongation of the coordinated IBr molecules in **3**·2IBr compared to those found in the solid state (solid state: 2.521 Å, $v = 216$ cm^{-1} [34,40]; gas phase: 2.470 Å, $v = 262$ cm^{-1} [41]; calculated, 2.505 Å, $v = 271$ cm^{-1} and 2.502 Å, $v = 270$ cm^{-1} at DFT and MP2 level, respectively). Accordingly, the FT-Raman frequencies reported for stronger CT-adducts between thioether [35] or thiocarbonyl and donors IBr [42,43] are correspondingly lower, falling in the ranges 166–184 and 144–147 cm^{-1}, respectively.

From the reactions of **1** with IBr in molar ratios ranging between 1:0.5 and 1:5 products featuring the same elemental analysis were isolated, whose stoichiometry corresponds to $(H1^+)I_2Br^-$. The FT-Raman spectrum features three peaks at 139, 120, and 82 cm^{-1}. Though two isomers of the I_2Br^- anion could exist [(I–I–Br)$^-$, $C_{\infty v}$; (I–Br–I)$^-$, $D_{\infty h}$], while the former type has been frequently reported [44], to the best of our knowledge only one example of the latter type has been structurally characterised [45]. In addition, the $C_{\infty v}$ isomer has been calculated (DFT/mPW1PW) to be more stable than the $D_{\infty h}$ one by about 5.5 kcal/mol. In the FT-Raman spectrum of $(H1^+)I_2Br^-$, the presence of three peaks excludes the presence of the symmetric (I–Br–I)$^-$ anion ($D_{\infty h}$ point group), and the three peaks could be assigned to the antisymmetric and symmetric stretching and π-deforming modes either of a (I–I–Br)$^-$ (corresponding normal modes calculated at 155, 124, and 67 cm^{-1} at MP2 level, Table 3), or of an asymmetric (I–Br–I)$^-$ anion.

In the case of the reactions of **2** with IBr, only one type of product was isolated whose elemental analysis

was in agreement with a stoichiometry of the anion close to $I_3Br_4^-$. The FT-Raman spectrum shows an envelope of peaks between 180 and 230 cm^{-1}, with three maxima at 186, 213, and 223 cm^{-1}, respectively. This allows to hypothesise the polyhalides as formed by a Br^- anion interacting with three perturbed IBr molecules, as recently found in the salt $(Ph_4P^+)(I_3Br_4^-)$ [46]. Unfortunately, notwithstanding numerous attempts, no crystals suitable for X-ray diffraction analysis were obtained to confirm the nature of the $I_3Br_4^-$ anion.

Finally, the reactions of **1–3** with ICl yield in all cases the protonated N-bases counterbalanced by ICl_2^- anions, with the only exception of **1** which, in 1:0.5 and 1:1 molar ratios, yielded $(H1^+)Cl^-$, characterised by X-ray diffraction (see above). For the three salts $(H1^+)ICl_2^-$, $(H_2 2^{2+})(ICl_2^-)_2$, and $(H_2 3^{2+})(ICl_2^-)_2$, only two FT-Raman peaks were observed at about 85 and 270 cm^{-1}, thus indicating a structural analogy for the three anions. On the basis of the almost symmetric nature of the ICl_2^- anion, structurally identified in the case of $(H_2 3^{2+})(ICl_2^-)_2$ (Fig. 3), the peaks can be tentatively attributed to the π_u bending (calculated at about 110 cm^{-1}), and to the σ_g stretching (calculated at about 250 cm^{-1}; Table 3) vibrations, respectively. The assignment of the FT-Raman peak at 270 cm^{-1} is consistent with those previously reported in the case of salts of the type $[L_2I^+]ICl_2^-$ (**L** = 2-methylpyridine and 1,10-phenanthroline, for which the reported Raman peak positions were 265 and 269 cm^{-1}, respectively) [47,48].

3. Conclusions

The reactivity towards I_2, Br_2, IBr and ICl of three pyridyl donors, namely *N*-ethyl-*N*′-3-pyridyl-imidazolidine-4,5-dione-2-thione (**1**), *N,N*′-bis(3-pyridylmethyl)-imidazolidine-4,5-dione-2-thione (**2**), and tetra-2-pyridyl-pyrazine (**3**), bearing one, two, and four pyridyl substituents, respectively, has been investigated and both crystal structure determinations and FT-Raman spectroscopy have been exploited for the understanding of the nature of the products isolated in the solid state. In all cases, such reactivity involved the pyridyl substituents, even when thiocarbonyl groups were available (compounds **1** and **2**), as a direct consequence of the scarce donor ability of thio- and seleno-carbonyl groups in thio- and seleno-parabanic acid derivatives [29]. As previously ascertained for other pyridyl donors, two different types of behaviour have been encountered, yielding either CT-adducts or pyridinium cations balanced by halide or polyhalide anions. The former type of products was found when **3** was reacted with I_2 and IBr. However, the majority of the isolated products belongs to the latter class of products instead. Analogously

to what proposed for pyridine, protonated cations may derive from solvolysis or reaction with incipient moisture of radical cations, generated by halogen oxidation. In the case of **3**, having four independent pyridyl substituents at the 1,3-diazine core, mono-, bi-, and tetra-protonated cations have been characterised in the salts $(H\mathbf{3}^+)Br_3^-$, $(H_2\mathbf{3}^{2+})(ICl_2^-)_2$, and $(H_4\mathbf{3}^{4+})(Br_4^{2-})$ $(Br^-)_2$, respectively.

As regards the anions, when crystals suitable for X-ray diffraction analysis were not available, the joined use of FT-Raman spectroscopy and elemental analysis, along with high-level theoretical calculations performed on the possible halide anions, allowed their identification, though in the case of the I_2Br^- and $I_3Br_4^-$ anions, the structural features of the polyhalides could only be hypothesised.

Finally, on the basis of the existing literature, of the results reported in this paper, and of the recent structural characterisation of $(H_4\mathbf{3}^{4+})(Br_4^{2-})(Br^-)$ [8], pyridyl donors seem to represent an interesting class of molecules, able to stabilise a great variety of different polyhalide anions in fascinating 2D and 3D supramolecular networks, suggesting that the complex frame of possible solid-state architectures, widely investigated for polyiodides [1,2,5,6], can be extended to all homo- or heteropolyhalides.

4. Experimental

4.1. General considerations

All solvents and reagents were purchased from Aldrich and used without further purification; $CHCl_3$ was distilled freshly over $LiAlH_4$ prior to use. All reactions were carried out under a dinitrogen atmosphere using standard vacuum line techniques. Elemental analyses were performed on a FISONS EA-1108 CHNS-O instrument. Infrared spectra were recorded on a Bruker IFS55 spectrometer at room temperature, purging the sample cell with a flow of dried air. Polythene pellets with a mylar beam-splitter and polythene windows (500–50 cm^{-1}, resolution 2 cm^{-1}) and KBr pellets with a KBr beam-splitter and KBr windows (4000–400 cm^{-1}, resolution 4 cm^{-1}) were used. FT-Raman spectra, in the range 500–50 cm^{-1}, were recorded with a resolution of 2 cm^{-1} on a Bruker RFS100 FT-Raman spectrometer, fitted with an In–Ga–As detector (room temperature) operating with a Nd-YAG laser (excitation wavelength 1064 nm), with a 180° scattering geometry. Tetra-2-pyridyl-pyrazine was synthesised according to literature methods [30]. The CH_2Cl_2 solutions of halogens and interhalogens were previously titrated by suspending 1 mL of solution in 50 mL of bidistilled water,

adding an excess of KI, and titrating with a standard solution of sodium thiosulphate 0.01 M with a Metrohm 776 Dosimat automatic buret.

4.2. Synthesis of N-ethyl-N′-3-pyridyl-thiourea

An isopropyl alcohol solution (30 mL) of ethylisothiocyanate (3.7 mL, 43 mmol) in was added drop wise, under a dinitrogen atmosphere, to a solution of 3-aminopyridine, (4 g, 43 mmol) in the same solvent (30 mL) at room temperature over a period of 2 h. The solution was stirred at room temperature for 12h. The solvent was removed under reduced pressure to yield a white powder (6.2 g, 79%). M.p. 115–116 °C. Elemental Anal. Calc. for $C_8H_{11}N_3S$: C, 53.01; H, 6.12; N, 23.18; S, 17.69%. Found: C, 53.01; H, 5.92; N, 23.20; S, 16.71%. Solid state FT-IR: 3141s, 2973s, 1533s, 1526s, 1477m, 1460m, 1421m, 1393w, 1369w, 1327m, 1269s, 1231m, 1206m, 1145m, 1094ms, 1053m, 1012m, 942m, 796w, 703w, 555w, 485w, 435w, 400s, 323s, 286s, 229s, 199w, 185w, 137s, 96s, 67s cm^{-1}. FT-Raman spectrum (20 mW; relative intensities in parentheses, strongest = 10): 323.5 (0.9), 124.6 (3.8), 100.1 (6.6), 80.61 (10.0) cm^{-1}s.

4.3. Synthesis of N-ethyl-N′-3-pyridyl-imidazolidine-4,5-dione-2-thione (1)

A solution of oxalyl chloride (1.4 mL, 16 mmol) in $CHCl_3$ (50 mL) was added drop wise, under a dinitrogen atmosphere, to a solution of *N*-ethyl-*N*′-3-pyridyl-thiourea, (2.9 g, 16 mmol) and triethylamine (4.4 mL, 32 mmol) in the same solvent (100 mL) at 0 °C, over a period of 5 h. The solution was refluxed for 8 h and then stirred at room temperature for 12h. The solvent was removed under reduced pressure and the solid residue dissolved in chloroform. The organic solution was washed with water (3 × 20 mL) and dried over Na_2SO_4. The solution was refluxed for 1 h with charcoal and, after hot filtration through Celite, the solvent removed under reduced pressure to yield a yellow powder (3.2 g, 79%). M.p. 200–204 °C. Elemental Anal. Calc. for $C_{10}H_9O_2N_3S$: C, 51.05; H, 3.86; N, 17.86; S, 13.63. Found: C, 51.02; H, 4.06; N, 17.67; S, 13.84%. Solid state FT-IR: 3502w, 3097m, 3065s, 2970w, 2872w, 2313m, 2070m, 1954m, 1778s, 1758s, 1609m, 1558m, 1474s, 1422s, 1371s, 1284s, 1201m, 1173s, 1088m, 1059w, 1036m, 1023m, 960m, 855w, 819m, 789m, 721m, 679m, 651m, 618m, 566m, 516w, 500m, 487m, 407s, 378s, 349s, 331s, 286w, 266m, 232m, 218w, 184w, 160m, 110m, 92m, 85m, 68w cm^{-1}. FT-Raman spectrum (20 mW; relative intensities in parentheses, strongest = 10): 517.2 (5.2), 497.2 (2.4), 342.7 (1.4), 125.1 (6.6), 103.2 (10.0), 74.8 (4.8), 58.8 (5.5) cm^{-1}.

4.4. Synthesis of N,N′-bis(3-pyridylmethyl)-imidazolidine-4,5-dione-2-thione (2)

2 was synthesised according to the procedure outlined for **1**, starting from oxalyl chloride (0.7 mL, 7.7 mmol) and 1,3-bis(3-pyridylmethyl)-2-thiourea (2.0 g, 7.7 mmol). Yield: 2.3 g, 61%. M.p. 153–155 °C. Elemental Anal. Calc. for $C_{15}H_{12}N_4O_2S$: C, 57.68; H, 3.87; N, 17.94; S, 10.26. Found: C, 58.08; H, 3.68; N, 17.75; S, 9.19%. Solid state FT-IR: 3501s, 2947s, 2361m, 1911w, 1773s, 1757s, 1591s, 1578s, 1477s, 1431s, 1414s, 1389s, 1348s, 1325s, 1252s, 1213s, 1190s, 1128m, 1103m, 1028s, 951m, 932m, 833s, 789s, 708s, 621m, 565m, 492m, 469m, 446s, 397s, 338s, 276s, 241w, 225w, 205m, 191m, 163w, 133s, 116m, 103m, 86m, 68w cm^{-1}. FT-Raman spectrum (50 mW; relative intensities in parentheses, strongest = 10): 205.5 (2.4), 87.8 (10.0), 72.8 (6.6), 61.5 (4.8) cm^{-1}.

4.5. Reactions of 1–3 with Br₂, I₂, IBr, and ICl

All products were obtained according to the following procedure: a CH_2Cl_2 solution of a weighted amount of **1–3** was reacted with a previously titrated CH_2Cl_2 solution of the halogen or interhalogen in 1:0.5, 1:1, 1:2, and 1:5 molar ratios. The solution was allowed to slowly air evaporate. After few days, the solid product was separated and washed with light petrolum ether (b.p. 40–60 °C).

4.5.1. (H1⁺)I₅⁻ (obtained from 1 and I₂)
M.p. 100–102 °C (decomposition). Elemental Anal. Calc. for $C_{10}H_{10}N_3O_2SI_5$: C, 13.79; H, 1.16; N, 4.83; S, 3.68. Found: C, 13.34; H, 1.75; N, 4.59; S, 3.58%. Solid state FT-IR: 486w, 474m, 438s, 420s, 384s, 353m, 325s, 302s, 289s, 280m, 270m, 255s, 247m, 228m, 203m, 195m, 176m, 171s, 151s, 140s, 95m, 85m, 68m cm^{-1}. FT-Raman spectrum (50 mW; relative intensities in parentheses, strongest = 10): 160.2 (10.0), 111.4 (4.8) cm^{-1}.

4.5.2. (H1⁺)Br⁻ (obtained from 1 and Br₂ in 1:0.5 and 1:1 molar ratios)
M.p. 245–247 °C. Elemental Anal. Calc. for $C_{10}H_{10}N_3O_2SBr$: C, 37.99; H, 3.19; N, 13.29; S, 10.12. Found: C, 37.87; H, 3.25; N, 13.19; S, 9.85%. Solid state FT-IR: 488m, 438m, 403s, 392s, 340s, 325s, 261m, 235s, 186s, 162s, 145s, 136s, 114s, 96m, 85m, 61m cm^{-1}. FT-Raman spectrum (200 mW; relative intensities in parentheses, strongest = 10): 342.0 (1.6), 261.7 (1.0), 118.9 (9.7), 97.1 (10.0), 72.9 (7.8) cm^{-1}.

4.5.3. (H1⁺)Br₅⁻ (obtained from 1 and Br₂ in 1:2 and 1:5 molar ratios)
M.p. 161–163 °C. Elemental Anal. Calc. for $C_{10}H_{10}N_3O_2SBr_5$: C, 18.89; H, 1.59; N, 6.61; S, 5.04.

Found: C, 19.03; H, 1.68; N, 6.98; S, 4.90%. Solid state FT-IR: 486w, 454m, 426s, 382m, 360s, 321s, 284s, 250m, 183s, 161s, 146s, 136s, 129m, 114m, 102m, 95s, 85s, 65s cm^{-1}. FT-Raman spectrum (200 mW; relative intensities in parentheses, strongest = 10): 175.9 (9.9), 160.2 (10.0), 78.3 (2.7) cm^{-1}.

4.5.4. (H1⁺)I₂Br⁻ (obtained from 1 and IBr)
M.p. 210–211 °C. Elemental Anal. Calc. for $C_{10}H_{10}N_3O_2SI_2Br$: C, 21.07; H, 1.77; N, 7.37; S, 5.62. Found: C, 21.48; H, 1.11; N, 7.40; S, 5.71%. Solid state FT-IR: 492s, 453m, 425m, 382m, 358s, 347m, 320s, 295m, 284s, 247m, 218w, 176s, 159s, 148s, 136s, 116m, 95m, 85m, 62m cm^{-1}. FT-Raman spectrum (50 mW; relative intensities in parentheses, strongest = 10): 139.2 (5.7), 119.8 (10.0), 82.1 (1.9) cm^{-1}.

4.5.5. (H1⁺)Cl⁻ (obtained from 1 and ICl in 1:0.5 and 1:1 molar ratios)
M.p. 218–220 °C. Elemental Anal. Calc. for $C_{10}H_{10}N_3O_2SCl$: C, 44.20; H, 3.71; N, 15.46; S, 11.78. Found: C, 44.73; H, 3.40; N, 15.60; S, 11.00%. Solid state FT-IR: 488s, 439s, 390s, 362m, 322m, 298m, 286w, 260s, 236s, 218m, 185s, 163s, 155s, 144s, 136s, 112s, 95s, 84m, 65s cm^{-1}. FT-Raman spectrum (50 mW; relative intensities in parentheses, strongest = 10): 343.0 (2.8), 124.4 (8.1), 102.5 (10.0), 59.7 (4.8) cm^{-1}.

4.5.6. (H1⁺)ICl₂⁻ (obtained from 1 and ICl in 1:2 and 1:5 molar ratios)
M.p. 141–143 °C. Elemental Anal. Calc. for $C_{10}H_{10}N_3O_2SICl_2$: C, 27.67; H, 2.32; N, 9.68; S, 7.39. Found: C, 27.31; H, 2.25; N, 9.08; S, 7.66%. Solid state FT-IR: 492s, 426m, 386w, 360m, 322m, 284m, 249m, 183s cm^{-1}. FT-Raman spectrum (50 mW; relative intensities in parentheses, strongest = 10): 271.5 (10.0), 184.4 (0.1), 84.9 (5.7) cm^{-1}.

4.5.7. (H2⁺)I₃⁻ (obtained from 2 and I₂)
M.p. 173–175 °C. Elemental Anal. Calc. for $C_{15}H_{13}N_4O_2SI_3$: C, 25.96; H, 1.89; N, 8.07; S, 4.62 Found: C, 26.00; H, 1.78; N, 7.93; S, 4.03%. Solid state FT-IR: 484s, 419m, 385s, 326m, 302m, 280s, 267m, 255m, 247m, 227m, 203m, 195m, 176s, 172m, 150s, 140s, 132s, 121s, 100s, 90s, 75s, 68s, 52w cm^{-1}. FT-Raman spectrum (150 mW; relative intensities in parentheses, strongest = 10): 115.4 (10.0), 63.9 (0.9) cm^{-1}.

4.5.8. (H2⁺)Br₅⁻ (obtained from 2 and Br₂)
M.p. 138–140 °C. Elemental Anal. Calc. for $C_{15}H_{13}N_4O_2SBr_5$: C, 25.27; H, 1.84; N, 7.86; S, 4.50. Found: C, 25.33; H, 2.62; N, 7.76; S, 4.44%. Solid state FT-IR: 566s, 484m, 445w, 413s, 365s, 319s, 309s, 271s, 236m, 217m, 163s, 145s, 136s, 128s, 114s, 95s, 84s, 67s cm^{-1}. FT-Raman spectrum (150 mW; relative intensities

in parentheses, strongest = 10): 190.6 (10.0), 156.6 (8.3), 103.5 (5.7), 81.4 (6.5) cm^{-1}.

4.5.9. $(H2^+)(I_3Br_4)^-$ (obtained from 2 and IBr)

M.p. 130–132 °C. Elemental Anal. Calc. for $C_{15}H_{13}N_4O_2SI_3Br_4$: C, 17.77; H, 1.29; N, 5.53; S, 3.16. Found: C, 17.57; H, 1.68; N, 5.59; S, 3.75%. Solid state FT-IR: 484m, 378s, 325s, 303s, 281s, 230m, 203s, 178s, 151s, 135s, 110s, 85s, 66m, 52w cm^{-1}. FT-Raman (500–50 cm^{-1}, relative intensities in parentheses, strongest = 10): 222.7 (6.6), 213.2 (6.6), 186.4 (10.0) cm^{-1}.

4.5.10. $(H2^+)(ICl_2^-)_2$ (obtained from 2 and ICl)

M.p. 118–120 °C. Elemental Anal. Calc. for $C_{15}H_{14}N_4O_2SI_2Cl_4$: C, 25.38; H, 1.99; N, 7.89; S, 4.51. Found: C, 26.47; H, 1.61; N, 8.23; S, 4.63%. Solid state FT-IR: 484m, 423m, 385s, 321m, 286m, 221m, 183s, 80w cm^{-1}. FT-Raman spectrum (150 mW; relative intensities in parentheses, strongest = 10): 267.9 (10.0), 200.5 (6.6), 83.5 (8.0) cm^{-1}.

4.5.11. $(3 \cdot 2I_2) \cdot [(H3^+)I_3^-]$ (obtained from 3 and I_2)

M.p. 235–236 °C. Elemental Anal. Calc. for $C_{24}H_{17}N_6I_3 \cdot C_{24}H_{16}N_6I_4$: C, 34.60; H, 2.00; N, 10.09. Found: C, 34.51; H, 2.05; N, 9.51%. Solid state FT-IR: 419w, 404w, 364m, 310m, 286m, 262s, 234s, 218s, 161m, 144s, 115s, 84m, 67w cm^{-1}. FT-Raman spectrum (6 mW; relative intensities in parentheses, strongest = 10): 170.0 (10.0), 147.1 (5.7), 110.2 (4.1) cm^{-1}.

4.5.12. $(H3^+)Br_3^-$ (obtained from 3 and Br_2 in 1:0.5 and 1:1 molar ratios)

M.p. 228–230 °C. Elemental Anal. Calc. for $C_{24}H_{17}N_6Br_3$: C, 45.82; H, 2.57; N, 13.36. Found: C, 46.68; H, 2.72; N, 13.50%. Solid state FT-IR: 419w, 402s, 392s, 332s, 311s, 295m, 286m, 261m, 251m, 218m, 184s, 163s, 145s, 136s, 125s, 115s, 95m, 84m, 66s, 52m cm^{-1}. FT-Raman spectrum (50 mW; relative intensities in parentheses, strongest = 10): 159.9(10.0), 51.2 (1.4) cm^{-1}.

4.5.13. $3 \cdot 2IBr$ (obtained from 3 and IBr)

M.p. 228–230 °C. Elemental Anal. Calc. for $C_{24}H_{16}N_6I_2Br_2$: C, 35.94; H, 2.01; N, 10.48. Found: C, 36.09; H, 1.80; N, 10.35%. Solid state FT-IR: 445m, 439m, 416m, 407m, 319m, 293w, 260w, 251w, 239w, 198s, 163s, 145s, 109s, 94s, 62s, 53s cm^{-1}. FT-Raman spectrum (200 mW; relative intensities in parentheses, strongest = 10): 203.8 (10.0), 99.9 (2.0), 78.8 (2.4) cm^{-1}.

4.5.14. $(H_23^{2+})(ICl_2^-)_2$ (obtained from 3 and ICl)

M.p. 225–226 °C. Elemental Anal. Calc. for $C_{24}H_{18}N_6I_2Cl_4$: C, 36.67; H, 2.31; N, 10.69. Found: C, 36.21; H, 2.25; N, 10.45%. Solid state FT-IR: 446w, 439s, 387s, 302s, 280s, 255s, 248s, 228s, 203m, 195m, 176s, 171m, 150s, 140s, 122s, 105s, 86m, 68m, 52w cm^{-1}. FT-Raman spectrum (28 mW; relative intensities in parentheses, strongest = 10): 567.6 (0.6), 487.9 (0.6), 409.7 (0.6), 294.4 (1.7), 267.0 (10.0), 169.1 (1.0), 148.7 (1.9), 86.0 (6.6) cm^{-1}.

4.6. X-ray crystal structure analysis

Data collection was performed at 120(2) K on a Bruker Nonius area detector diffractometer with Mo-Kα radiation ($\lambda = 0.71073$ Å). An absorption correction was applied using the SADABS V2.10 algorithm [49]. The structure was solved by direct methods and refined on F^2 by using the SHELX program [50,51] implemented in the WinGX suite [52]. Anisotropic displacement parameters were assigned to all non-hydrogen atoms. Hydrogen atoms were included in the structure using the riding model.

4.7. Theoretical calculations

Density functional theory (DFT) and second order Møllet–Plesset (MP2) calculations were performed with the GAUSSIAN 98 program package [53] on the isolated molecules and anions listed in Table 3. In all cases, normal mode frequency calculations were performed at the optimised geometries. Based on the results recently reported on donor-acceptor interactions between dithiolene donors [M(R,R'timdt)$_2$] (M = Ni, Pd, Pt; R,R'timdt = formally monoreduced form of disubstituted imidazolidine-2,4,5-trithione) and halogens [54], DFT calculations were performed using Adamo's and Barone's mPW1PW functional [55], while the LanL2DZ basis set with ECP [56,57] was used for all calculations, with the addition of diffuse and polarisation functions (LanL2DZdp) [58], thus obtaining slightly better optimised geometries and vibrational frequencies with respect to those previously reported.

5. Supplementary material

Crystallographic data for **1**, $(H1^+)Br^-$, $(H1^+)Cl^-$, $(H2^+)I_3^-$, **3 · 2IBr**, and $(H_23^{2+})(ICl_2^-)_2$ have been deposited with the Cambridge Crystallographic Data Centre as supplementary publication no. CCDC 249255, 249256, 249257, 249259, 249254, and 249258, respectively. Copy of the data can be obtained free of charge on application to CCDC, 12 Union Road, Cambridge CB2 1EZ, UK [fax (int) +44 1223 336 033; e-mail: deposit@ccdc.cam.ac.uk]. Optimised geometries, orbital energies, and vibrational data for all compounds listed in Table 3 are available from the authors on request.

Acknowledgements

References

[1] M.C. Aragoni, M. Arca, F.A. Devillanova, A. Garau, F. Isaia, V. Lippolis, G. Verani, Coord. Chem. Rev. 184 (1999) 271.

[2] H. Svensson, L. Kloo, Chem. Rev. 103 (2003) 1649.

[3] M.C. Aragoni, M. Arca, F. Demartin, F.A. Devillanova, A. Garau, F. Isaia, V. Lippolis, S. Rizzato, G. Verani, Inorg. Chim. Acta 357 (2004) 3803.

[4] K.-F. Tebbe, R. Buchem, Angew. Chem., Int. Ed. 36 (1997) 1345.

[5] A.J. Blake, F.A. Devillanova, R.O. Gould, W.-S. Li, V. Lippolis, S. Parson, C. Radeck, M. Schröder, Chem. Soc. Rev. 27 (1998) 195.

[6] M.C. Aragoni, M. Arca, F.A. Devillanova, M.B. Hursthouse, S.L. Huth, F. Isaia, V. Lippolis, A. Mancini, Cryst. Eng. Comm. 6 (2004) 540.

[7] K.O. Strømme, Acta Chem. Scand. 13 (1959) 2089.

[8] M.C. Aragoni, M. Arca, F.A. Devillanova, M.B. Hursthouse, S.L. Huth, F. Isaia, V. Lippolis, A. Mancini, H. Ogilvie, Inorg. Chem. Commun. 8 (2005) 79–82.

[9] K.N. Robertson, P.K. Bakshi, T.S. Cameron, O. Knop, Z. Anorg. Allg. Chem. 623 (1997) 104.

[10] M.C. Aragoni, M. Arca, F.A. Devillanova, F. Isaia, V. Lippolis, A. Mancini, L. Pala, A.M.Z. Slawin, J.D. Woollins, Chem. Commun. (2003) 2226.

[11] P. Deplano, F.A. Devillanova, J.R. Ferraro, F. Isaia, V. Lippolis, M.L. Mercuri, Appl. Spectrosc. 46 (1992) 1625.

[12] P. Deplano, J.R. Ferraro, M.L. Mercuri, E.F. Trogu, Coord. Chem. Rev. 188 (1999) 71.

[13] E.L. Rimmer, R.D. Bailey, W.T. Pennington, T.W. Hanks, J. Chem. Soc., Perkin Trans. 2 (1998) 2557.

[14] R. Bailey Walsh, C.W. Padgett, P. Metrangolo, G. Resnati, T.W. Hanks, W.T. Pennington, Cryst. Growth Des. 1 (2) (2001) 165.

[15] R.D. Bailey, M.L. Buchanan, W.T. Pennington, Acta Crystallogr. C 48 (1992) 2259.

[16] R.D. Bailey, G.W. Drake, M. Grabarczyk, T.W. Hanks, L.L. Hook, W.T. Pennington, J. Chem. Soc., Perkin Trans. 2 (1997) 2773.

[17] R.D. Bailey, M. Grabarczyk, T.W. Hanks, W. Pennington, J. Chem. Soc., Perkin Trans. 2 (1997) 2781.

[18] E.L. Rimmer, R.D. Bailey, T.W. Hanks, W.T. Pennington, Chem. Eur. J. 22 (2000) 4071.

[19] S. Aroson, P. Epstein, D.B. Aroson, G. Wieder, J. Phys. Chem. 86 (1982) 1035.

[20] O. Hassel, H. Hope, Acta Chem. Scand. 15 (1961) 407.

[21] S. Aronson, P. Epstein, D.B. Aronson, G. Wieder, J. Phys. Chem. 86 (1982) 1035.

[22] S. Soled, G.B. Carpenter, Acta Crystallogr. B 30 (1974) 910.

[23] A. Parlow, H. Hard, Z. Naturforsh. B 40 (1985) 45.

[24] M.C. Aragoni, M. Arca, F. Demartin, F.A. Devillanova, A. Garau, F. Isaia, V. Lippolis, G. Verani, Trends Inorg. Chem. 6 (1999) 2.

[25] M.C. Aragoni, M. Arca, F. Demartin, F.A. Devillanova, A. Garau, F. Isaia, F. Lelj, V. Lippolis, G. Verani, Chem. Eur. J. 7 (2001) 3123.

[26] M.C. Aragoni, M. Arca, A.J. Blake, F.A. Devillanova, W.-W. du Mont, A. Garau, F. Isaia, V. Lippolis, G. Verani, C. Wilson, Angew. Chem. Int. Ed. 40 (2001) 4229.

[27] M.C. Aragoni, M. Arca, F. Demartin, F.A. Devillanova, A. Garau, P. Grimaldi, F. Isaia, F. Lelj, V. Lippolis, G. Verani, Eur. J. Inorg. Chem. 2363 (2003).

[28] Although **1** and **2** contain thiocarbonyl groups, which could possibly compete with the pyridyl nitrogens in interacting with halogens and interhalogens, their donor ability is so low that it was impossible to determine the stability constant of N,N'-dimethy-limidazolidine-4,5-dione-2-thione adduct with diiodine [29].

[29] M. Arca, F. Demartin, F.A. Devillanova, F. Isaia, F. Lelj, V. Lippolis, G. Verani, Can. J. Chem. 78 (2000) 1147.

[30] H.A. Goodwin, F. Lions, J. Am. Chem. Soc. 81 (1959) 6415.

[31] It is worth noting that in the case of the products obtained from the reactions between pyridyl donors and halogens or interhalo-gens, FT-IR spectroscopy is not of great help in investigating the nature of the compounds isolated in the solid state. In fact, whatever the reaction product (adduct or N-protonated donor balanced by halide or polyhalide anions), the MIR spectrum is very similar to that of the starting donor, the only difference being the presence of the NH stretching band, occurring under protonation. As far as the FIR region is regarded, much more information is gained from FT-Raman spectroscopy.

[32] W. Ried, G.W. Broft, J.W. Bats, Chem. Ber. 116 (1983) 1547.

[33] P. Brix, J. Voss, G. Adiwidjaja, J. Chem. Res. 94 (1994) 618.

[34] L.N. Swink, G.B. Carpenter, Acta Crystallogr. B 24 (1968) 429.

[35] A.J. Blake, F.A. Devillanova, A. Garau, F. Isaia, V. Lippolis, S. Parsons, M. Schröder, J. Chem. Soc., Dalton Trans. (1999) 525.

[36] M. Graf, H. Stoekli-Evans, Acta Crystallogr. C 52 (1996) 3073.

[37] H. Bock, T. Vaupel, C. Näther, K. Ruppert, Z. Havlas, Angew. Chem. Int. Ed. Eng. 31 (1992) 299.

[38] P.H. Svensson, L. Kloo, J. Chem. Soc., Dalton Trans. (2000) 2449.

[39] F.H. Herbstein, M. Kapon, G.M. Reisner, Acta Crystallogr. B 41 (1985) 348.

[40] F. Cristiani, F. Demartin, F.A. Devillanova, F. Isaia, V. Lippolis, G. Verani, Inorg. Chem. 33 (1994) 6315.

[41] L.E. Selin, Naturwissenschaften 47 (1960) 104.

[42] N. Bricklebank, P.J. Skabara, D.E. Hibbs, M.B. Hursthouse, K.M.A. Malik, J. Chem. Soc., Dalton Trans. (1999) 3007.

[43] P.J. Skabara, N. Bricklebank, R. Berridge, S. Long, M.E. Light, S.J. Coles, M.B. Hursthouse, J. Chem. Soc., Dalton Trans. (2000) 3235.

[44] See for example O.J. Dautel, M. Formigue, E. Canadell, Chem. Eur. J. 7 (2001) 2635.

[45] T. Naito, A. Tateno, T. Udagawa, H. Kobayashi, R. Kato, A. Kobayashi, T. Nogami, J. Chem. Soc., Faraday Trans. 90 (1994) 763.

[46] R. Minkwitz, R. Berkei, R. Ludwig, Inorg. Chem. 40 (2001) 25.

[47] G.A. Bowmaker, K.–H. Tan, M.J. Taylor, Aust. J. Chem. 33 (1980) 1743.

[48] At this regard, it is interesting to observe that in ICl_2^- ions the symmetric σ_g stretching mode is calculated to fall at higher energy than the antisymmetric σ_u one, because in centrosymmetric $D_{\infty h}$ trihalides on passing from I_3^-, to IBr_2^-, to ICl_2^-, the σ_g mode increases in energy more than the σ_u mode. In fact, while the σ_g mode involves only the motion of the terminal atoms and the central iodine atom remains still, the antisymmetric σ_u stretching mode involves the motion of the central heavy iodine atom and therefore is less affected by the change in the terminal atoms.

[49] G.M. Sheldrick, SADABS V2.10, 2003.

[50] G.M. Sheldrick, Acta Crystallogr. A 46 (1990) 467.

[51] G.M. Sheldrick, SHELX-97, Program for Crystal Structure Refine-ment, University of Göttingen, Germany, 1997.

[52] L.J. Farrugia, J. Appl. Crystallogr. 32 (1999) 837.

[53] M.J. Frisch, G.W. Trucks, H.B. Schlegel, G.E. Scuseria, M.A. Robb, J.R. Cheeseman, V.G. Zakrzewski, J.A. Montgomery, R.E. Stratmann, J.C. Burant, S. Dapprich, J.M. Millam, A.D. Daniels, K.N. Kudin, M.C. Strain, O. Farkas, J. Tomasi, V. Barone, M. Cossi, R. Cammi, B. Mennucci, C. Pommeli,

C. Adoma, S. Clifford, J. Ochterski, G.A. Peterson, P.Y. Ayala, Q. Cui, K. Morokuma, D.K. Malick, A.D. Rabuck, K. Raghav-achari, J.B. Foresman, J. Cioslowski, J.V. Ortiz, B.B. Stefanov, G. Liu, A. Liashenko, P. Piskorz, I. Komaromi, R. Gomperts, R.L. Martins, D.J. Fox, T. Keith, M.A. Al-Lahan, C.Y. Peng, A. Nanayakkara, C. Gonzalez, M. Challacombe, P.M.W. Gill, B.G. Johnson, W. Chen, M.W. Wong, J.L. Andres, M. Head-Gordon, E.S. Replogle, J.A. Pople, GAUSSIAN 98 (Revision A.7), Gaussian Inc., Pittsburgh, PA, 1998.

[54] M.C. Aragoni, M. Arca, F. Demartin, F.A. Devillanova, F. Lelj, F. Isaia, V. Lippolis, A. Mancini, L. Pala, G. Verani, Eur. J. Inorg. Chem. (2004) 3099.
[55] C. Adamo, V. Barone, J. Chem. Phys. 108 (1998) 664.
[56] P.J. Hay, W.R. Wadt, J. Chem. Phys. 82 (1985) 299.
[57] J.V. Ortiz, P.J. Hay, R.L. Martin, J. Am. Chem. Soc. 114 (1992) 2736.
[58] J.M. Bailey, B.J. Wright, T.M. Gilbert, L.S. Sunderlin, J. Phys. Chem. A 105 (2001) 8111.